

Original Article

Machine Learning Regression Approaches for Prediction Microhardness of Al-Y₂O₃ Composite

Sachin Rathore¹, Ratnesh Kumar Raj Singh², K.L.A. Khan³

¹KIET Group of Institutions, Ghaziabad, AKTU Lucknow.

²Thapar Institute of Engineering and Technology, Patiala.

³Dean IEC, KIET Group of Institutions, Ghaziabad.

¹sachinrathoreme@gmail.com

Received: 10 March 2022

Revised: 20 April 2022

Accepted: 22 April 2022

Published: 26 April 2022

Abstract - The present study investigated the experimental analysis of microhardness of Al-Y₂O₃ composite material developed through the friction stir processing (FSP) route. The microhardness values were measured for a different set of experiments, and then these data were used for various machine learning (ML) models. All measured data sets were divided into two portions in which 75% of rules were used for training, and the remaining 25% of the data rules were used for testing the regression models. Experiments were carried out on various input parameters such as tool traverse speed (TS), Spindle speed (SS), number of passes and direction of rotation (tool). The micro-hardness data is considered as output response. The microhardness value increased 34.47% from BM, reaching a maximum of 147 HV on 1000rpm SS and 100 mm/min TS, with double pass FSP in which the direction of rotation of the tool is in the opposite direction. To predict microhardness values, various ML-regression algorithms have been considered, mainly: Fine tree (FT), Linear regression (LR), Interactions Linear regression (ILR), and Robust Linear regression (RLR), Stepwise Linear regression (SLR) and support vector machines (SVM). It is found that RLR generated appropriate prediction of microhardness with minimum errors based on measurement of Root Mean Square Error (RMSE), Error score (R2), Mean squared error (MSE) and mean absolute error (MAE).

Keywords - Friction stir processing, Machine learning, Support vector machine, Regression algorithm, Microhardness.

1. Introduction

According to society's demand, new products keep coming into the market, and this will continue forever. But nowadays, Safety is a major issue in the automotive, aviation and other transport industries. Every modern industry requires strong, lightweight, corrosion-resistant and cost-effective materials [1]. Aluminium-based alloys have the highest strength-to-weight ratio of any other metals. Thus, they are commonly suited to aerospace applications [2]. But Al alloys are less dense than steel alloys, leading to decreased strength and stiffness. Therefore, research's shown through their results that the mechanical properties of the Al alloy specimens could be improved by binding of reinforcement matrix [3]. Aluminium metal matrix composites (AlMMCs) are successfully accepted by industry due to their rigorous properties such as being light in weight, highly resistive to corrosion, wear resistance and cost-effective [4].

Stir Casting, infiltration, powder metallurgy, diffusion bonding, and spray deposition are major fabrication techniques for developing Al-MMCs [5]. But most of the

methods are muddled with high lead time. FSP is a pressurized heat, solid-phase surface modification process that combines the advantages of conventional solid-state deformation processes [6]. Friction stir welding (FSW) is the foundation of FSP's operation, which was developed in the early 1990s by the Battelle Memorial Institute and The Welding Institute (TWI) in the United Kingdom [7]. FSP is a process that uses a rotating tool to stir the material while it is being deformed. The tool is rotated at a constant speed, and the material is deformed at a constant rate [8]. FSP has been used to manufacture biomedical implants, aircraft components, light composite panels, sports goods, and many automotive, aircraft, military, and various industrial parts to improve their effectiveness and reduce the overall production cost [9].

In recants years, numerous researches have been published on the FSP process parameter's effects on microhardness, UTS, tribology and metallurgical behaviours [10]. In FSP, the most likely process parameters are tool pin profile [11], spindle rotation speed [12], traverse speed [13], shoulder diameter, number of passes [14] & tool tilt angles [15]. Luo X et al. [16] looked into the impact of double-pass



on elongation and fracture strength of AZ61 magnesium alloy by the FSP route. They observed the processing of the composite improved the surface modification, resulting in an increase in UTS and ductility. Shojaeefard M et al. [17] The particle distribution in the B4C/aluminium composite manufactured with the square pin profile is more uniform than that in the composite fabricated using the hexagonal and cylindrical pin profiles. Kumar A. [18] The microstructural development, mechanical characteristics, and corrosion behaviour of the FSPed alloy plates were examined using FSP on Al 7075 alloy at varied traverse speeds and spindle rpm. The results revealed that when the traverse (mm/min) and spindle speed (rpm) increased, the microstructure of the FSPed alloy plates got finer. The alloy sheet's tensile strength, elongation, and corrosion resistance improved as the traverse rate, and spindle speed increased.

The data obtained from these works are the fuel for new research and innovation. The more data you have, the more insights can be generated and the better proofing of your research. Machine learning (ML) is commonly used in the research field. The ML is a method of training machines to learn from past rules without being categorically programmed. Predictive modelling is a branch of ML used to predict future events [19]. ML can be classified into 3 types: supervised, unsupervised, and reinforcement learning. Regression analysis is a branch of machine learning that deals with the problem of predicting the value of a continuous variable. The type of regression analysis determines the type of linear relationship between the two variables. The Support Vector Machine (SVM) algorithm is a supervised learning algorithm used for classification and regression. Numerous researchers have adopted ML and artificial intelligence (AI) techniques to predict the various properties of MMCs. In this way, Banerjee T. et al. [20] used an Artificial neural network (ANN) to predict & optimized the tribological properties of Al composite. Jun Liu et al. [21] demonstrated the effect of elastic constant and UTM on graphene reinforced aluminium (Gr/Al) nanocomposites by SVM and ANN models. Shozib I. et al. [22] developed a prediction algorithm on ML to optimize the microhardness of TiO₂ composite.

In this study, some machine learning algorithms were developed to predict the microhardness of fabricated aluminium composite. Fine Tree, linear, interactions, robust, stepwise, SVM regression models optimize the dependent variables concerning several errors. Almost 240 experimental data sets were incorporated with mentioned ML models. The data set is divided into 75% and 25% for training and testing, respectively. For the present research work, the fabrication of composite through the FSP route and the effect of process variables on microhardness is explained in section 2. The implementation of the ML algorithm, regression analysis, error calculations and modelling are described in section 3. Finally, section 4 is devoted to a conclusion.

2. Materials and Method

2.1 Fabrication of Surface Composite

The aluminium 2219 alloy is mainly used to produce aircraft parts, particularly for the airframe and landing gear. This is because the AA2219 alloy has high strength and high corrosion resistance. This alloy has been widely used in the aerospace industry for many years since it has high tensile strength and can withstand harsh environments. Yttrium aluminium garnet is a composite with good wear and thermal shock resistance. It can be used for making electrodes and linings in high-temperature furnaces. Yttrium is very hard and refractory and does not react with water and air. It has a high melting point of 3290°C and thus is used in military and industrial applications where heat resistance is needed. Thus, in this research, an attempt has been made to develop an aluminium-yttrium composite material by the FSP route.

The underwater FSP improves the corrosion resistance of the substrate. The low-temperature frictional deformation enhances the Al-yttrium oxide (AA2219-Y₂O₃) composite hardness and wears resistance. The non-conductive nature of water prevents electrochemical reactions from occurring between the tool & composite plate. When the material is being processed in FSP, it is crucial to understand two important parameters, i.e., TRS & TTS. When changing these two variables together, there can be significant changes in the properties of processed materials. The heat generated in the film stack is highly dependent on the thickness of the thermal barrier and thermal resistance coefficient. The heat generated will also decrease with a decrease in the TTS and increase in TTS, respectively, affecting the grains, depending on the desired to get the desired properties in an FSPed material to optimize the TRS & TTS. The dimensions of the Al plates were 200 mmx50mmx6mm. The mechanical properties and chemical composition of alloy material are shown in Tables 1 & 2.

Table 1. Chemical composition of AA2219 alloy

Element	Cu	Mn	Zr	V	Ti	Al
Wt. (%)	6.3	0.3	0.18	0.1	0.06	Balance

Table 2. Mechanical properties of AA2219 alloy

Material	Yield strength (MPa)	Ultimate tensile strength (MPa)	Elongation (%)	Vickers hardness (0.5 kg)
Base Material	310	408	23	140

Three longitudinal circular holes were drilled on an aluminium plate with 3 mm diameter and 180mm length at the centre of the plate. The hole was filled with Y₂O₃ powder as a reinforcement particle. All holes are evenly spaced,

which creates an even distribution of material throughout the plates for added strength. Fabrication of surface metal matrix composite, Al 2219 alloy in plate structure as a base material and yttrium oxide (Y_2O_3) particles were used as a reinforcement with an average size between 67 to 123 μm as measured from SEM. For making the composite, the weight percentage of Y_2O_3 was taken at 10% because it provided the highest ratio of tensile strength to elongation as obtained from the trial experiment.

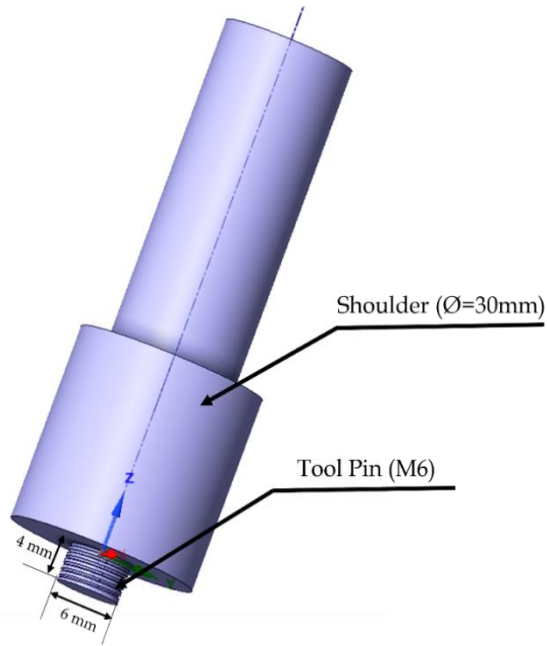


Fig. 1 Schematic diagram of the FSP H13 tool used for this study

A non-consumable tool with a unique material H13 hot-die steel design, with shoulder diameter of 30 mm and external right hand threaded (M6) pin of 4 mm length as shown in figure 1. Preparation of surface composite was carried out on a Vertical milling centre (VMC) made by Jyoti CNC Automation Limited, and the tool shoulder pressure was kept constant for all specimens. Experiments were performed with a 2-degree tilt angle from the y-axis. The process input parameters applied for these experiments included different spindle speeds in rpm, four traverse speeds, and the different number of passes. A schematic diagram showing the overall setup is shown in figure 2(a, b).

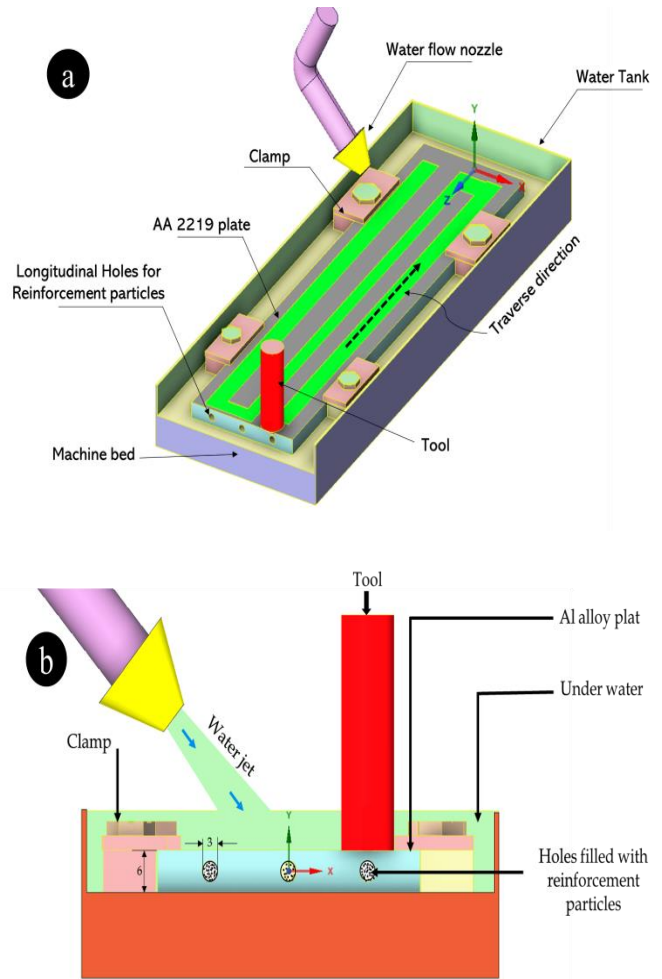


Fig. 2 Schematic diagram of underwater FSP
(a) Isometric view of setup with the double-pass tool
(b) End view of longitudinal holes

The FSP of the composite plate has been done with various combinations of machine parameters along with variable tool number of passes and direction of rotation, as presented in table 3. The literature review sets the ranges of all input parameters. Production of FSPDs composite, the tool rotation speed has three levels 600, 1200 & 1600 rpm with different traverse speeds 60, 100 & 140 mm/min. The rotating speed of the stirring tool in a processing zone has a significant effect on the stirring action. It improves the properties of that stir zone up to a certain limit, but after that point, it causes defects to form due to high turbulence. After FSP, specimens for testing were sliced from the stir zone, as shown in fig. 3, and these samples were cut by the wire cut EDM (make CAM-TECH ENGINEERS). Specimen dimensions and preprocessing as per ASTM standard.

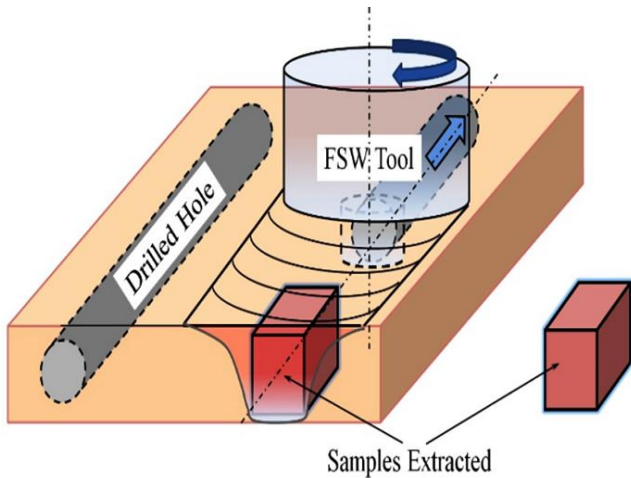


Fig. 3 Schematic illustration of FSP & hardness samples extraction

3. Experimental Results

3.1 Microstructural characterization

Exerted, polished and etched the specimens using a mixture of hydrochloric acid, hydrofluoric & nitric acids (180 millilitres distilled water, 3.5 ml Hydrochloric acid, 2 ml HF (hydrofluoric acid) & 5 ml HNO₃ (nitric acid)). A scanning electron microscope (SEM) is used to look at the surface of an object, whereas optical microscopy is used to measure the interior. Optical microscopy (OM) and scanning electron microscopy (SEM) investigated the grain characterization, particle distribution, and overall microstructure. Figure 4 (a, b) shows the grain refinement and dispersion of reinforcement particles on single and Double passes of the FSP tool on the Al plate.

3.2 Microhardness Hardness

The average hardness of as-received AA2219 aluminium was 140 HV. The microhardness of AA2219 and Al-Y₂O₃ composite samples were tested according to the ASTM standard test method. Vickers hardness tester (Leco LM 248 AT) was used by applying a force of 100 grams for 10 seconds as a dwell time on the substrates. The hardness measurement was observed 3 times for each specimen in different locations, and average values were taken for microhardness.

In specimen FSPed without mixing reinforcement particles, compared with as-received material, the average hardness value increased and reached the maximum of 78 HV in the processed zone. Statement to the Hall-Petch relationship, the hardness of the material is proportional to the temperature and stress applied to the material. Here reduction of grain size increases the value of hardness [24]. The process of annealing is used to improve the properties of a material. On the other hand, the temperature rise during FSP anneals material in a stirred zone.

The existence of reinforcement in the aluminium matrix and the quench hardening effect is caused by variations in the aluminium matrix's thermal contraction coefficient. And Y₂O₃ particles [25]. The annealing action can reduce hardness, referring to Fig. 4(a, b); consistency improvement in hardness can be responsible for uniformity of reinforced particles dispersion after FSP, which gives rise to a more influential distribution of hardening. Further, dislocation density and substantial grain refinement are also responsible for enhancing the hardness. Maximum hardness was achieved with the fabrication of Y₂O₃ particles (maximum 147 HV) due to severe grain size reduction, as shown in fig. 4(a, b). The uniform distribution of particles in the aluminium matrix and the presence of a higher number of Y₂O₃ particles in the composite layer.

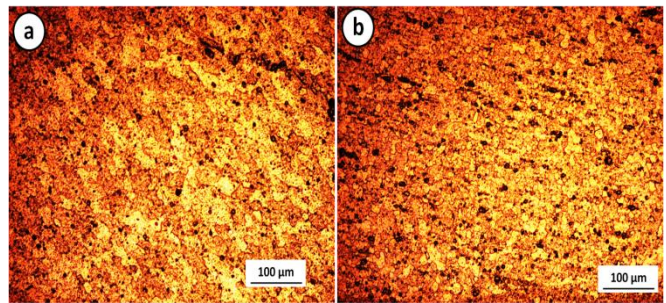


Fig. 4 SEM images of Fraction stir processed zone at 1000 rpm (SS), 100 mm/min (TS) on: (a) Single pass same direction (SPSD) (b) Double pass opposite direction (DPOD) [23]

4. Effect of Process Parameters

Fig. 5(a, b) illustrates the effect of tool rotation speed (RPM) on FSPed Al-Y₂O₃ surface composite. Various research investigated the effects of FSP process parameters on mechanical and metallurgical properties of Al-composites, already discussed in the introduction section. For this study, only four process parameters were considered to determine and optimize the effect on hardness interconnection to material characterization, whose details are as follows:

4.1 Spindle Speed

The hardness of the processed zone is shown in Fig. 5 (a) and 5(b) concerning traverse speed and tool rotation direction. Here the microhardness of the stir zone has been improved from 67 HV to 147 HV on 1000 RPM at the Double pass-opposite direction (DPOD) due to refinement of the grain size and strain hardening. Modification of surface due to proper heat distribution and pressure; therefore, the Y₂O₃ reinforcement particles were fully penetrated in the base alloy. According to the Hall-Petch scientific relationship, the strength of a processed Composite is proportional to the square root of its particle size [26]. The relationship is based on the idea that as the grain size decreases, its strength increases. This is because smaller grains have a higher surface-to-volume ratio and are more

susceptible to defects and fracture. But the hardness of the processed material doesn't need to increase with spindle speed. It is often observed that it decreases after a range of spindle speed [27], mainly due to the porosity of the processed composite material, which is generated due to excessive heat. As seen in the figure, it is natural to fall after 1000 rpm from 147 HV to 132 HV; this decrement of hardness is due to the rate of overheating.

4.2 Traverse Speed Effect

The hardness value of fabricated composites was measured after various experiments. The hardness is simultaneously increased concerning the increment of traverse speed. The maximum microhardness value has reached the maximum of 100 mm/min at DPOD. The hardness improvement is 37.47% compared to SPSD at 60 mm/min, as shown in Fig.5 (a-b). It is not always true that the hardness of a material is increased by increasing the traverse speed. The hardness may be decreased if the speed is too high; consider the stagnation point, which arrived after 110mm/min on every combination. The gradual increment of

traverse speed leads to particle size reduction, and age hardening increases Al alloy's hardness [28]. Therefore, the hardness of Al has been increased concerning the traverse speed.

4.3 No of pass & Tool direction of rotation

After measuring the hardness of FSP Al composites, it was observed that increment of the no of the pass also improves the material hardness. Fig. 5 (a-b) shows the hardness comparison with the reference of single and double passes. The hardness value has been increased in the double pass, the same direction from 67 HV to 83 HV on 60 mm/min (TS) and 500 rpm (SS). A 7.86 % improvement in hardness was observed compared with the single-pass opposite direction (SPOD) at 1000 rpm (SS). The tool double pass-FSP has been refining and spheroidized the particle size of Y2O3, also dispersed with base material; therefore, hardness has been increased. However, after 1000 rpm (SS), the hardness does not increase due to strain hardening and decrement of interfacial bonding [29].

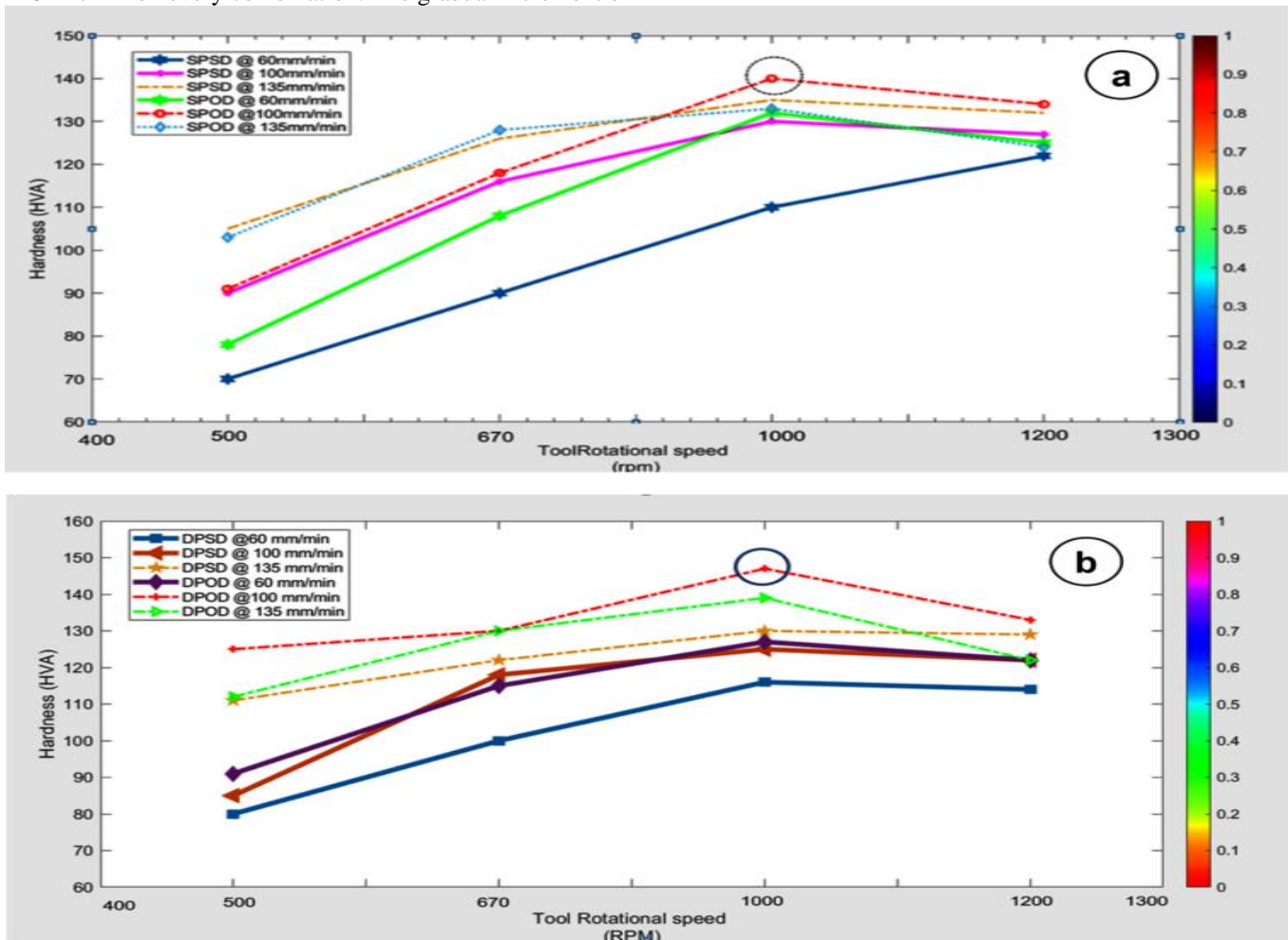


Fig. 5 Effect of tool rotation speed on microhardness of FSPed composite on various traverse speeds with same and opposite direction of the tool on (a) single pass (b) Double pass

5. Machine Learning Approaches

A few different machine learning approaches can be implemented on MATLAB. One approach uses a pre-trained model, such as a deep neural network to predict a target variable. Another approach is to use a machine learning algorithm, such as a support vector machine or a neural network, to learn a model that can predict the target variable. This paper applied all prediction methodologies on MATLAB under a supervised machine learning approach.

Regression analysis is a widely used predictive modelling technique. However, as present data becomes more complex, it is hard to analyze relationships between the variables and come up with a concrete prediction [30]. Here one dependent variable is hardness, and four independent variables are spindle speed, traverse speed, no of pass & spindle direction of rotation.

The Support Vector Machine (SVM) algorithm is a supervised learning algorithm used for classification and regression. The algorithm is a type of kernel machine learning algorithm, and it is a popular technique used in data mining and machine learning. The SVM algorithm works by finding a hypersurface in the feature space that separates the data into two or more classes. The SVM algorithm can be used for both classification and regression. In regression, the input features are used to predict the value of a given variable [31].

For the present study, six-regression machine learning algorithms were considered to predict the hardness as a dependent variable. All types of machine learning approaches were conducted @ MATLAB R2021a. Some steps are following:

5.1 Step 1: Load the data into MATLAB

Machine learning needs the training data set in matrix form to generate the prediction models. The table shows all input and output data as per machine language.

Equation for normal & logical linear regression analysis is:

$$y = p1*x + p2 \text{ -----(1)}$$

- y= Prediction or target (Dependent variable)
- p1= independent (explanatory) variable
- p2= intercept
- x= coefficient or residual

for prediction of the hardness of the multiple variable linear equations:

$$hardness (y)=m1*Rotational speed +m2*Traverse speed+m3*No of Pass+m4* Direction Of rotation +b ----(2)$$

Dependent variable= "Hardness"
 Independent variable (Features)= "Rotational speed, Traverse speed, no of the pass, Direction of rotation."

Table 3 shows the various models and their dependent/independent variables and coefficients for perfect fitting; all values were developed with the help of the Machine learning application toolbox @MATLAB R2021a. As per MATLAB linguistic machine language, all independent data sets have been converted into various matrix levels.

5.2 Step 2: Convert the Data to a Matrix & Run the Regression Analysis on Various Models

In this step, all variables were applied through the MS-excel sheet by the command window on the MATLAB toolbox. Here 48 rows and 5 columns of data (48*5) were considered a matrix, predicting the dependent variables. Afterload the entire data, run the regression analysis with the help of a machine learning application built with MATLAB toolbox in terms of 75:25 training and testing data. A cross-validation method is a technique used to estimate the accuracy of a predictive model by dividing the data into training and validation sets, learning the model on the training set, and then testing the model on the validation set. Here 4 folds of cross-validation & fine Tree with 4 leaves were assumed on MATLAB for better results. All selection was due to optimized linear regression, available on the machine learning toolbox. Table 4 shows the summary of all models concerning linear regression.

Table 3. Input/output data variables for machine learning algorithms

variable		Level/Range	Matrix
Independent (Features)	Rotational speed (rpm)	500	1
		670	2
		1000	3
		1600	4
	Traverse speed (mm/min)	60	1
		100	2
		135	3
	No of Pass	Single	1
Double		2	
Direction of Rotation	Same	1	
	Opposite	2	
Dependent	Hardness (HVA)	67-147	67-147

Table 4. Summary of regression models

Model	Regression Equation	p1	p2	Norms of residual
Fine Tree	$y = p1 * x + p2$	0.84339	18.9053	44.354
Linear		0.96865	3.6971	20.9325
Interactions Linear		0.98419	1.3774	26.1713
Robust Linear		1.0066	-0.8427	14.789
Stepwise Linear		0.96819	3.7523	20.6969
Linear SVM		0.93415	8.0265	22.8205

5.3 Step 3: Result plotting

After all algorithm iterations, the prediction data set was exported through the model export tab. A 3D surf graph was drawn between traverse speed and rotation speed and their effect on hardness. The red-coloured area of the 3-D surface plot Fig. 6 exhibits the plot's maximum height and represents the maximum value of microhardness. This surface area demonstrates the prediction value of microhardness which was optimized through machine learning algorithm - regression analysis models.

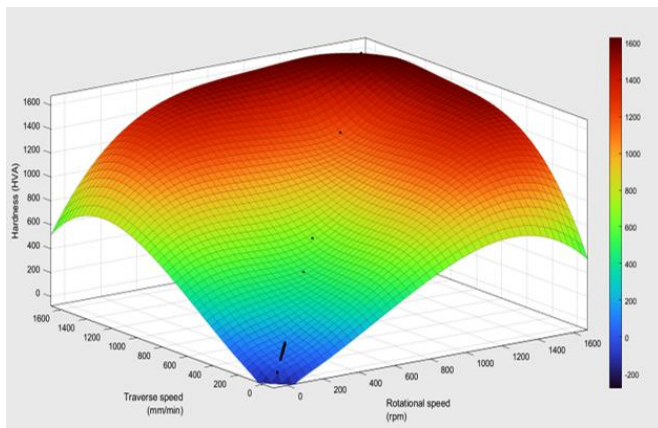


Fig. 6 3-D Surfacer Plot shows the effect of traverse speed and rotation speed on microhardness response

All experimental and prediction values are shown in Fig. 7. The blue-coloured points represent the true experimental values of microhardness, and the yellow-coloured dots represent the prediction values of microhardness on a 2D scatter plot. All prediction dots are obtained by various regression models on training data sets. Fig. 8 represents the scatter diagram of the independent variable. The actual or experimental value of the micro-hardness acts on the horizontal axis, whereas the predicted value of hardness

flows on the vertical axis. The experimental vales were measured by a Vickers hardness tester (LM-247 AT). In contrast, the predictive values of microhardness were analyzed through ML regression models, mainly FT, LR, ILR, RLR, SLR and SVM. All scatter plots are drawn through the plotting toolbox on MATLAB. The yellow-coloured inclined line is the perfect prediction line; on that line, all experimental points are equal to prediction points. Another black line represents the best statistical prediction curve with linear regression equation on the scatter diagrams for all six ML models.

5.4 Step 4: Models comparison based on error Index

The values of the machine learning model, evaluation performance metrics, and various types of errors have been shown in Table 5 to compare the models' errors and forecast the microhardness. The entire dataset containing 48 data rules was used for the models, where 36 data rules (75%) were selected as training data, and the remaining 12 data rules (25%) were used as testing samples for output prediction evaluation. After validation, identified the perfect model with the help of RSME, R², MSE & MAE. All types of errors, as shown in Table 5

5.5 RMSE (Root Mean Squared Error)

The model with the lowest MSE is the one that most accurately predicts the data. The minimum value of RMSE means a better connection between experimental and prediction values during training and testing. The bar graph Fig. 9(a) shows the RMSE value of various models. Fig. 9(a) shows the RMSE value of various models. The ideal value for **R-square** is 1, which would indicate that the model perfectly explains the variation in the data. However, real-world datasets typically have r-squares that are much lower than 1.

5.5.1 The Mean Square Error (MSE)

The Mean Square Error (MSE) is a statistic used in regression analysis to measure the amount of error in a predicted value. The MSE is calculated by taking the sum of the squared differences between the predicted and actual values, divided by the number of data points. The ideal value for MSE in regression analysis is zero.

5.5.2 The Mean Absolute Error (MAE)

The Mean Absolute Error (MAE) is a statistic used to measure the accuracy of predictions made by a model. The MAE is calculated by taking the average absolute values of the differences between the actual and predicted values. The ideal value of MAE is zero.

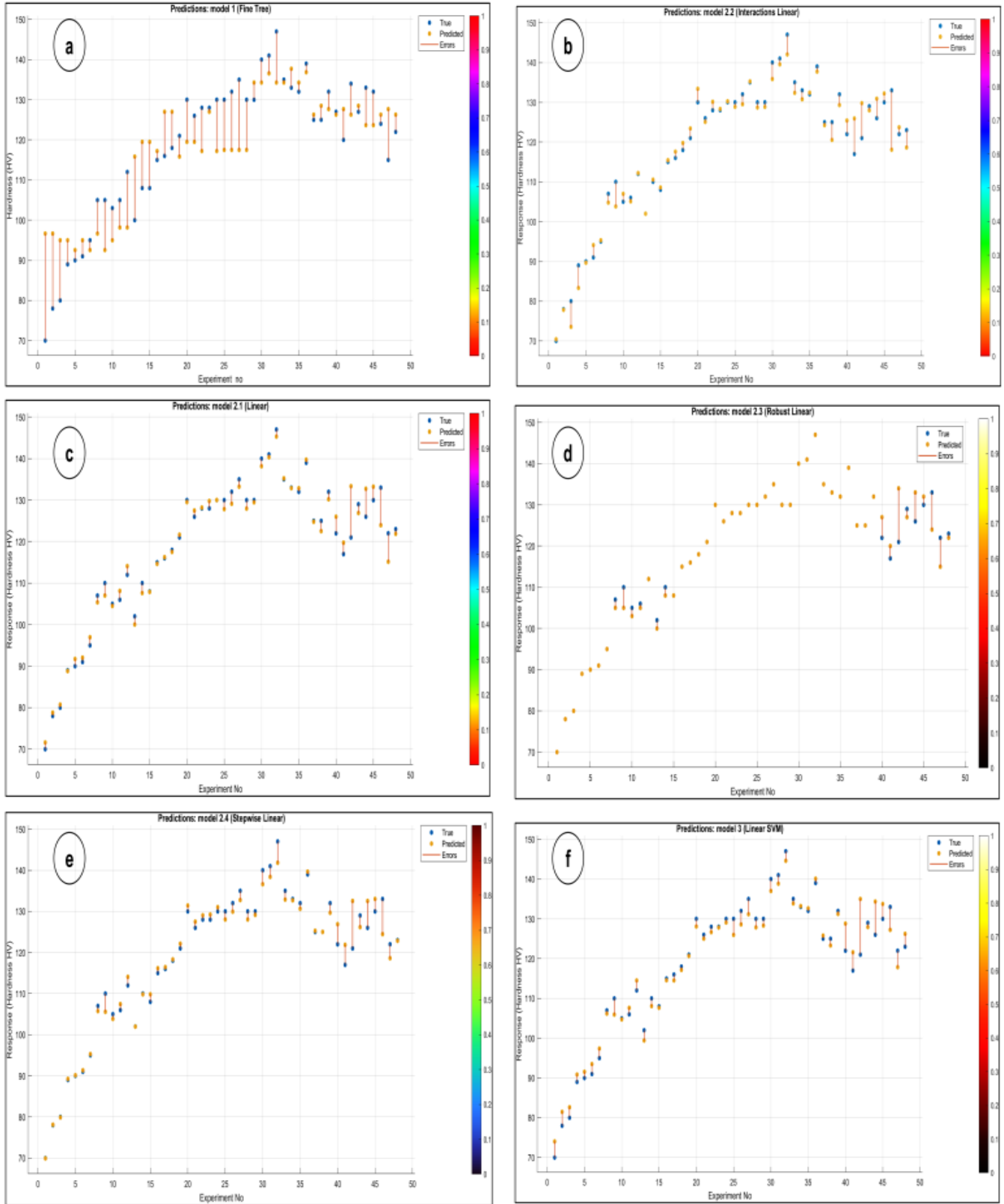


Fig. 7 True and predicted curve for microhardness for training data of (a) FT, (b) LR, (c) ILR, (d) RLR, (e) SLR, (f) SVM models

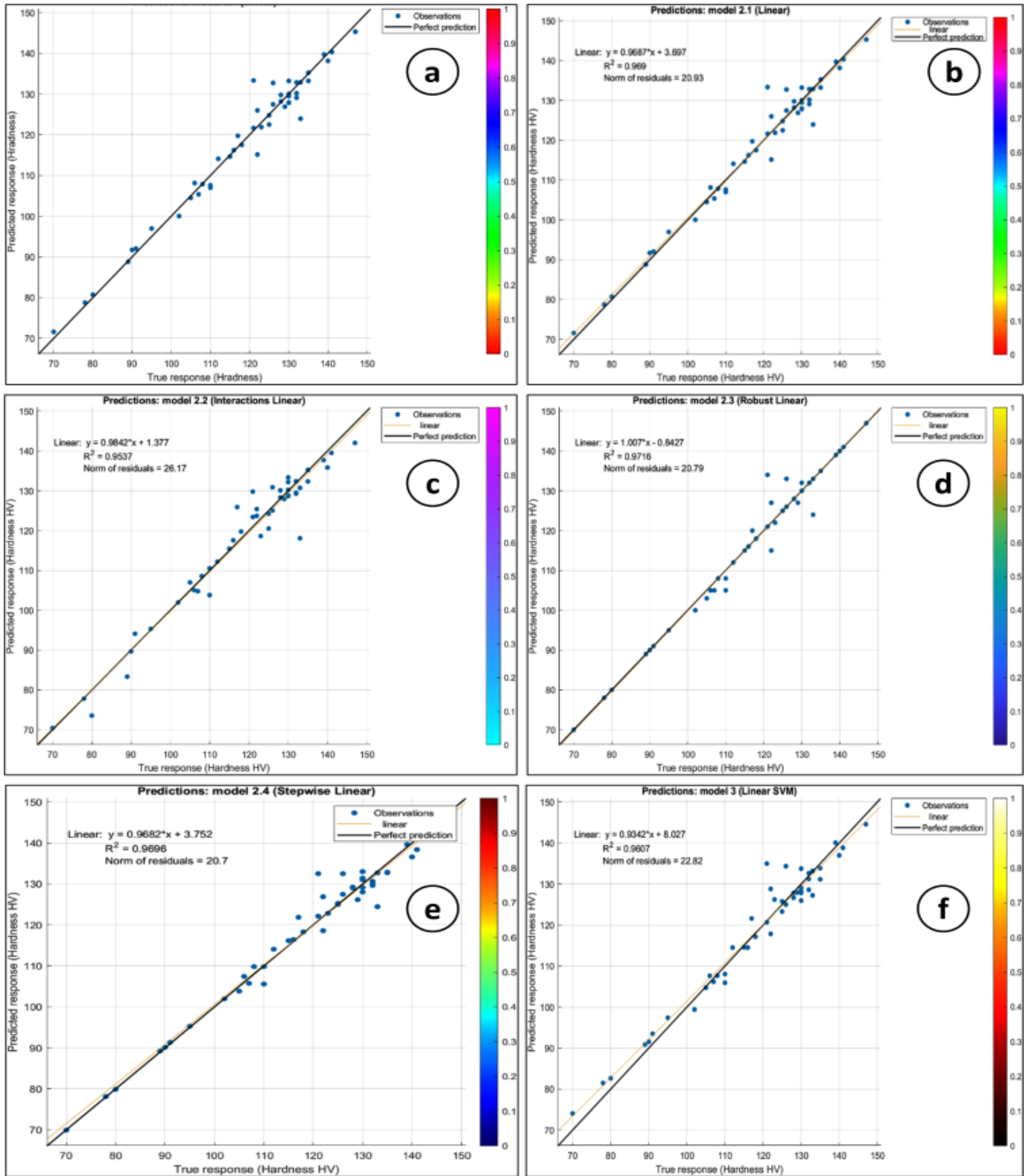


Fig. 8 Actual vs predicted curve for microhardness for Testing of (a) FT, (b) LR, (c) ILR, (d) RLR, (e) SLR, (f) SVM models

For the present study, the Robust linear regression model has a minimum RSME of 3.0035, 0.97 vales of R^2 , $0 < R^2 < 1$, minimum value MSE (3.234) and MAE (1.3125), as shown in Table: 5

Table 5

Model/ Algorithm		Fine Tree (FT)	Linear Regression (LR)	Interactions Linear (ILR)	Robust Linear (RLR)	Stepwise Linear (SLR)	Linear SVM (SVM)
RMSE	Training	6.967	3.0704	3.8201	3.004	3.0384	3.495
	Test	4.257	2.8098	2.4178	2.125	2.6613	2.967
R-Squared	Training	0.85	0.97	0.95	0.97	0.97	0.96
	Test	0.94	0.97	0.98	0.99	0.98	0.97
MSE	Training	48.54	9.4274	14.593	3.234	9.2321	12.21
	Test	81.12	7.8948	5.8456	2.747	7.0825	8.8
MAE	Training	5.287	1.9939	2.585	1.313	2	2.538
	Test	3.241	1.7499	1.6272	1.113	4.3938	1.96

A glimpse of all error types concerning machine learning models is shown in Fig. 9 (a-d). A bar graph fig. 9 (a) demonstrates the RSME values of six models by the performance of the training and test data set. The lower vale of RSME is better for prediction than other ML models. Now observe fig 9 (b); the FT model has the least value of R^2 , 0.85 (Training) and 0.94 (test), which is more suitable for the best prediction. However, observe the value of MSE and MAE from fig 9 (c-d), all values recommended for FT, LR, ILR, RLR, SLR and SVM models. Again, the bar distribution plot gives the least errors of the RLR model (3.234, 2.747), (1.3125, 1.1125) on training and test data sets.

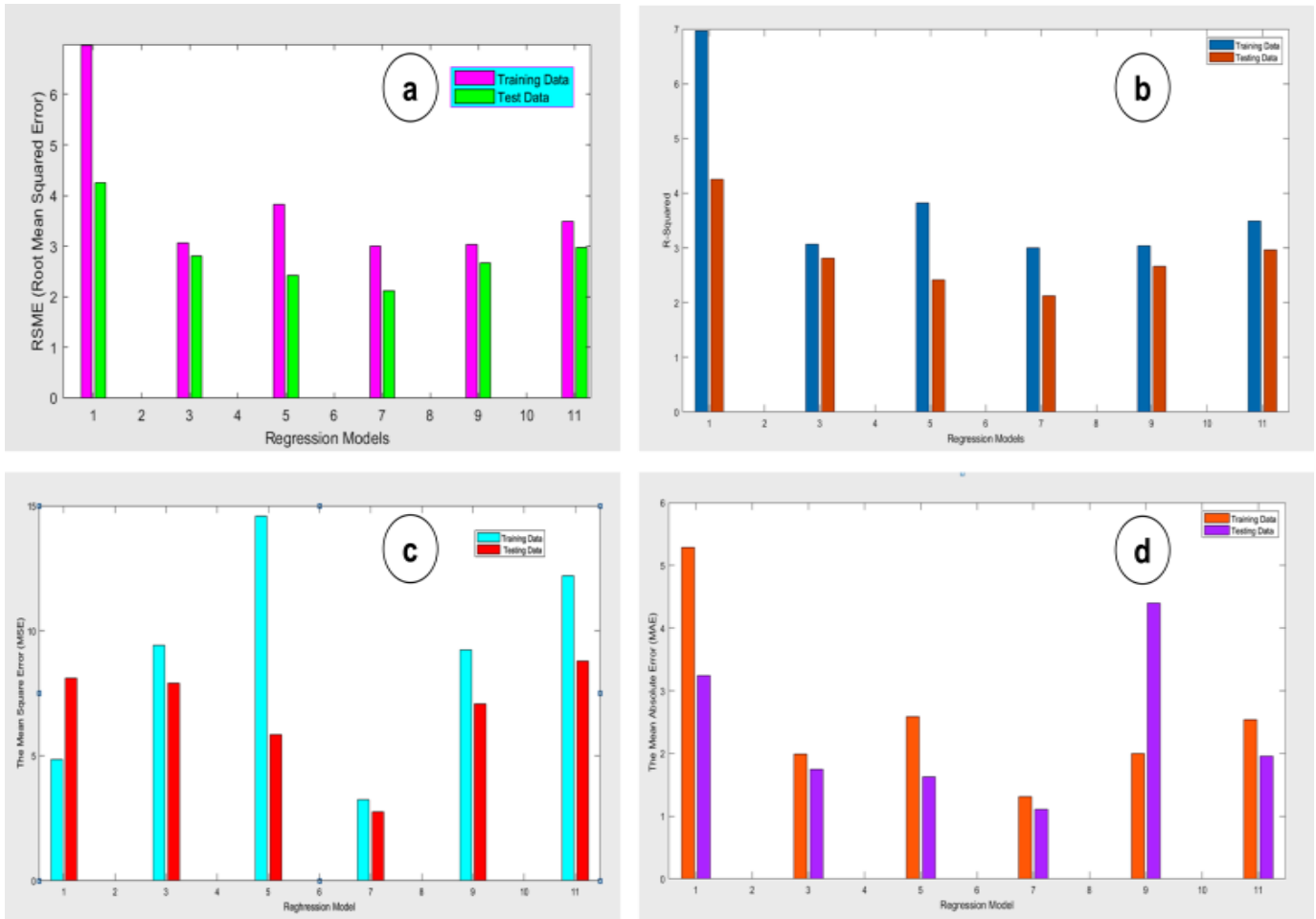


Fig. 9 Errors for six Machine learning models (a) RMSE, (b) R2, (c) MSE, (d) MAE

5.6 Hardness prediction based on the Robust Linear regression (RLR) model

In this study, six regression algorithms were applied to the machine learning toolbox on MATLAB to predict the hardness. Various types of errors, including RSME, R^2 , MSE and MAE, are shown in fig. 9. Based on the comparison of minimum error here, selection of RLR algorithm for prediction the hardness as a dependent variable. The RLR algorithm is designed to minimize the influence of outliers on the estimated relationship [32]. The prediction and actual results through the ML algorithm are shown in fig 9(a), While the other fig. 9(b) represents the error of the RLR model. According to this graph, the maximum error is +24 %/-10.5 %, placed at 120 HV. Although, its value at other points is less than 2 %, which represents the reconciliation between prediction and experiment value.

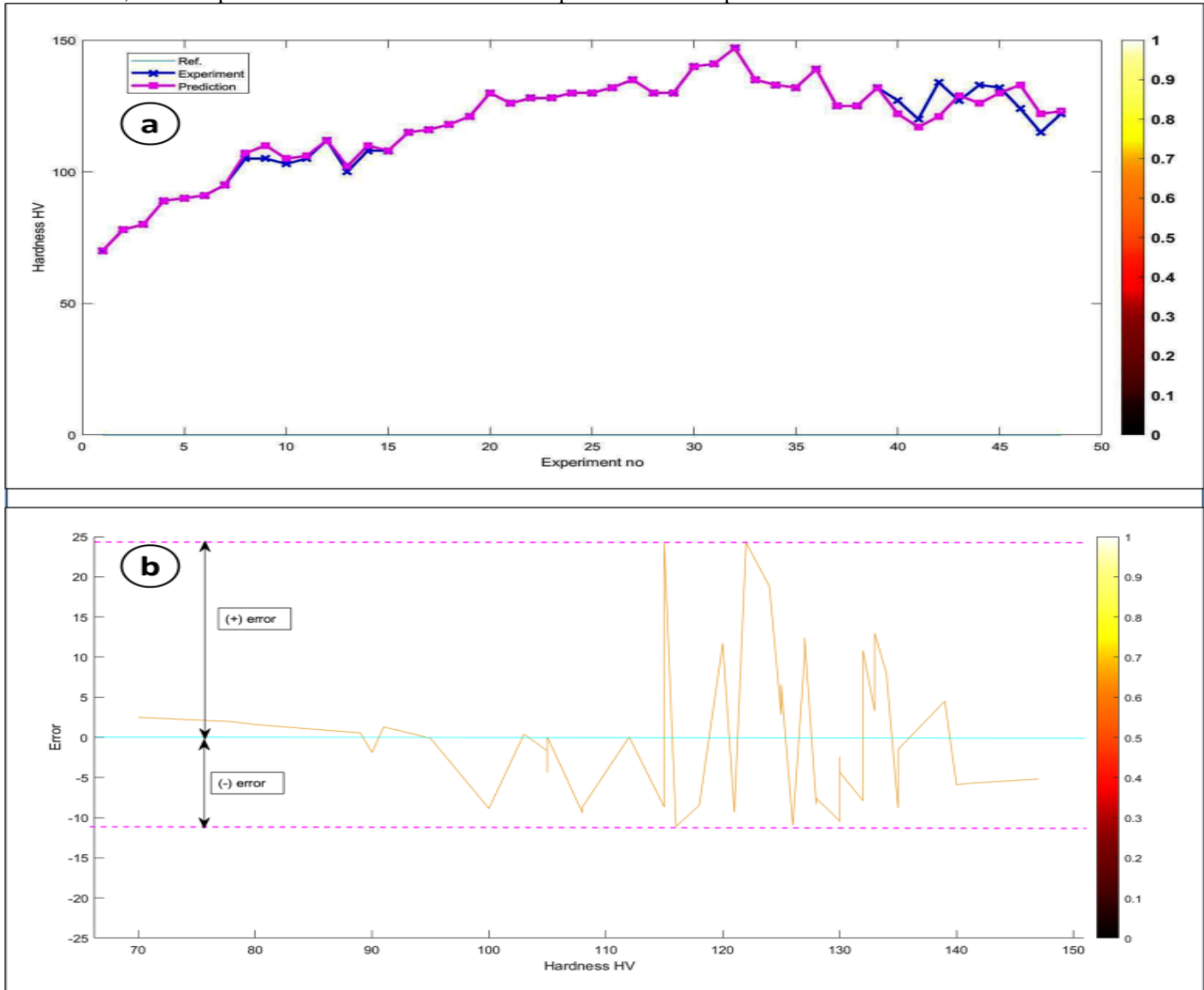


Fig. 10 a) comparison between experimental and prediction values of microhardness, b) Percentage of error for RLR model.

6. Conclusion

In the present paper, some machine learning models have been developed to predict the hardness of Al-Y₂O₃ composite produced through the FSP route. Six prediction models were based on a supervised ML approach (regression) and validated to the experimental dataset. Four input FSP parameters (spindle speed, traverse speed, no of passes and rotation direction) have been taken to optimize microhardness as a dependent variable. The major conclusion that can be drawn from this research is as follow:

- The value of microhardness prominently depends on all considered input variables, thoroughly verified by experiments and ML algorithms
- The microhardness value increased 34.47% from BM. The maximum microhardness value is 147 HV on 1000rpm (SS), 100 mm/min (TS), and DPOD.
- The improvement of the microhardness due to fine particles, heat input and cooling condition

- All experiment values were applied on ML to predict the microhardness under 75% training & 25 % training dataset.
- Robust Linear (RLR) model given the minimum errors between RSME, R^2 , MSE and MAE.
- Through the Robust linear regression prediction model, the maximum errors are $\pm 15\%$.
- The application of ML to predict and verify experimental data is very helpful for reducing the expense of testing for each specimen.

References

- [1] T. Dursun and C. Soutis, Recent developments in advanced aircraft aluminium alloys, *Materials and Design*, 56 (2014) 862–871. doi: 10.1016/j.matdes.2013.12.002.
- [2] J. Sarkar and S. Bhattacharyya, Application of graphene and graphene-based materials in clean energy-related devices Minghui, *Archives of Thermodynamics*, 33(4) (2012) 23–40. doi: 10.1002/er.
- [3] M. Manoharan and J. J. Lewandowski, Effect of reinforcement size and matrix microstructure on the fracture properties of an aluminum metal matrix composite, *Materials Science and Engineering A*, 150(2) (1992) 179–186. doi: 10.1016/0921-5093(92)90110-M.
- [4] Surappa M.K., *Aluminium Matrix Composites: Challenges and Opportunities // Sadhana. Department of Metallurgy, Indian Institute of Science, Bangalore 560 012, India*, 28(1-2) (2003) 319–334.
- [5] T. S. Srivatsan, I. A. Ibrahim, F. A. Mohamed, and E. J. Lavernia, Processing techniques for particulate-reinforced metal aluminium matrix composites, *Journal of Materials Science*, 26(22) (1991) 5965–5978. doi: 10.1007/BF01113872.
- [6] H. S. Arora, H. Singh, and B. K. Dhindaw, Composite fabrication using friction stir processing - A review, *International Journal of Advanced Manufacturing Technology*, 61(9–12) (2012) 1043–1055. doi: 10.1007/s00170-011-3758-8.
- [7] R. S. Mishra, Z. Y. Ma, and I. Charit, Friction stir processing: A novel technique for fabrication of surface composite, *Materials Science and Engineering A*, 341(1–2) (2003) 307–310. doi: 10.1016/S0921-5093(02)00199-5.
- [8] S. Wadekar, R. Soladhra, H. Barkade, and N. Thombare, A Review on Friction Stir Technology, *International Conference on Ideas, Impact and Innovation in Mechanical Engineering (ICIIME 2017)*, 5(6) (2017) 1542–1549.
- [9] Lucie Beth Johannes, friction stir processing for superplasticity and other applications. (2003) 1–50.
- [10] S. Rathore, R. K. R. Singh, and K. L. A. Khan, Effect of Process Parameters on Mechanical Properties of Aluminum Composite Foam Developed by Friction Stir Processing, *Proceedings of the Institution of Mechanical Engineers, Part B: Journal of Engineering Manufacture*, 235(12) (2021) 1892–1903. doi: 10.1177/09544054211021341.
- [11] K. Elangovan and V. Balasubramanian, Influences of tool pin profile and tool shoulder diameter on the formation of friction stir processing zone in AA6061 aluminium alloy, *Materials and Design*, 29(2) (2008) 362–373. doi: 10.1016/j.matdes.2007.01.030.
- [12] K. Elangovan and V. Balasubramanian, Influences of pin profile and rotational speed of the tool on the formation of friction stir processing zone in AA2219 aluminium alloy, *Materials Science and Engineering A*, 459 (2007) 7–18. doi: 10.1016/j.msea.2006.12.124.
- [13] H. Rana and V. Badheka, Elucidation of the role of rotation speed and stirring direction on AA 7075-B 4 C surface composites formulated by friction stir processing, *Proceedings of the Institution of Mechanical Engineers, Part L: Journal of Materials: Design and Applications*, 233(5) (2019) 977–994. doi: 10.1177/1464420717736548.
- [14] K. Nakata, Y. G. Kim, H. Fujii, T. Tsumura, and T. Komazaki, Improvement of mechanical properties of aluminum die casting alloy by multi-pass friction stir processing, *Materials Science and Engineering*, 437 (2006) 274–280. doi: 10.1016/j.msea.2006.07.150.
- [15] A. Kumar, S. K. Sharma, K. Pal, and S. Mula, Effect of Process Parameters on Microstructural Evolution, Mechanical Properties and Corrosion Behavior of Friction Stir Processed Al 7075 Alloy, *Journal of Materials Engineering and Performance*, 26(3) (2017) 1122–1134. doi: 10.1007/s11665-017-2572-3.
- [16] X. C. Luo, D. T. Zhang, G. H. Cao, C. Qiu, and D. L. Chen, Multi-pass submerged friction stir processing of AZ61 magnesium alloy: strengthening mechanisms and fracture behavior, *Journal of Materials Science* 54(11) (2019) 8640–8654. doi: 10.1007/s10853-018-03259-w.
- [17] M. H. Shojaeefard, M. Akbari, A. Khalkhali, and P. Asadi, Effect of tool pin profile on distribution of reinforcement particles during friction stir processing of B4C/aluminum composites, *Proceedings of the Institution of Mechanical Engineers, Part L: Journal of Materials: Design and Applications*, 232 (2018) 637–651. doi: 10.1177/1464420716642471.
- [18] A. Kumar, S. K. Sharma, K. Pal, and S. Mula, Effect of Process Parameters on Microstructural Evolution, Mechanical Properties and Corrosion Behavior of Friction Stir Processed Al 7075 Alloy, *Journal of Materials Engineering and Performance*, 26(3) (2017) 1122–1134, Mar. 2017, doi: 10.1007/s11665-017-2572-3.
- [19] A. Kordijazi, H. M. Roshan, A. Dhingra, M. Povolo, P. K. Rohatgi, and M. Nosonovsky, Machine-learning methods to predict the wetting properties of iron-based composites, *Surface Innovations*, 9(2-3) (2021) 111–119. doi: 10.1680/jsuin.20.00024.
- [20] T. Banerjee, S. Dey, A. P. Sekhar, S. Datta, and D. Das, Design of Alumina Reinforced Aluminium Alloy Composites with Improved Tribo-Mechanical Properties: A Machine Learning Approach, *Transactions of the Indian Institute of Metals*, 73(12) (2020) 3059–3069. doi: 10.1007/s12666-020-02108-2.
- [21] J. Liu, Y. Zhang, Y. Zhang, S. Kitipornchai, and J. Yang, Machine learning assisted prediction of mechanical properties of graphene/aluminium nanocomposite based on molecular dynamics simulation, *Materials & Design*, 213 (2022) 110334. doi: 10.1016/j.matdes.2021.110334.
- [22] I. A. Shozib et al., Modelling and optimization of microhardness of electroless Ni-P-TiO₂ composite coating based on machine learning approaches and RSM, *Journal of Materials Research and Technology*, 12 (2021) 1010–1025, 2021, doi: 10.1016/j.jmrt.2021.03.063.
- [23] S. Rathore, R. K. Raj Singh, and K. L. A. Khan, Artificial intelligent approach for process parameters modeling of friction stir processing, in *Materials Today: Proceedings*, 43 (2020) 326–334. doi: 10.1016/j.matpr.2020.11.671.
- [24] T. Rajmohan, K. Gokul Prasad, S. Jeyavignesh, K. Kamesh, S. Karthick, and S. Duraimurugan, Studies on friction stir processing parameters on microstructure and micro hardness of Silicon carbide (SiC) particulate reinforced Magnesium (Mg) surface composites, in *IOP Conference Series: Materials Science and Engineering*, 390(1) (2018) doi: 10.1088/1757-899X/390/1/012013.
- [25] H. Ahamed and V. Senthilkumar, Role of nano-size reinforcement and milling on the synthesis of nano-crystalline aluminium alloy composites by mechanical alloying, *Journal of Alloys and Compounds*, 505(2) (2010) 772–782. doi: 10.1016/j.jallcom.2010.06.139.
- [26] A. Kumar, K. Pal, and S. Mula, Simultaneous improvement of mechanical strength, ductility and corrosion resistance of stir cast Al7075-2% SiC micro- and nanocomposites by friction stir processing, *Journal of Manufacturing Processes*, 30 (2017) 1–13. doi: 10.1016/j.jmapro.2017.09.005.

- [27] P. Vijayavel and V. Balasubramanian, Effect of tool velocity ratio on tensile properties of friction stir processed aluminum-based metal matrix composites, *Journal of the Mechanical Behavior of Materials*, 25(3-4) (2016) 99–109. doi: 10.1515/jmbm-2016-0012.
- [28] T. Rajmohan, K. Gokul Prasad, S. Jeyavignesh, K. Kamesh, S. Karthick, and S. Duraimurugan, Studies on friction stir processing parameters on microstructure and micro hardness of Silicon carbide (SiC) particulate reinforced Magnesium (Mg) surface composites, in *IOP Conference Series: Materials Science and Engineering*, 390(1) (2018). doi: 10.1088/1757-899X/390/1/012013.
- [29] K. Nakata, Y. G. Kim, H. Fujii, T. Tsumura, and T. Komazaki, Improvement of mechanical properties of aluminum die casting alloy by multi-pass friction stir processing, *Materials Science and Engineering A*, 437(2) (2006) 274–280. doi: 10.1016/j.msea.2006.07.150.
- [30] W. ben Chaabene, M. Flash, and M. L. Nehdi, Machine learning prediction of mechanical properties of concrete: Critical review, *Construction and Building Materials*, 260 (2020). doi: 10.1016/j.conbuildmat.2020.119889.
- [31] E. Messele Sefene, A. A. Tsegaw, and A. Mishra, Process parameter optimization of Friction Stir Welding on 6061AA using Supervised Machine Learning Regression-based Algorithms.
- [32] Mohammed. A. Z. & D. S. Tauqir Nasir a, Applications of Machine Learning to Friction Stir Welding Process Optimization, *Jurnal Kejuruteraan*, 32(2) (2020) 171–186. doi: 10.17576/jkukm-2020-32(2)-01.